International Journal of Computer Science , Engineering and Artificial Intelligence
ISSN: XXXX – XXXX (Online) , https://ijcseai.com/
Regular Issue, Vol. 3, Issue. 2 (April – June) , 2026 , Pages: 7 - 14
Received: 21 August 2025 ; *Accepted:* 07 April 2026 ; *Published:* 18 April 2026
https://doi.org/10.63328/IJCSEAI-V3RI2P2
https://www.youtube.com/watch?v=Gjiz1wHMg-k
Original Paper : Applied Research – Experimental Research Paper

Quantum Kernel Learning for Emotion Recognition Using EEG

Surya Pavan Kumar Gudla

Department of Computer Science and Engineering, Aditya Institute of Technology and Management, Tekkali Andhra Pradesh, India 532201;

** Corresponding Author: Surya Pavan Kumar Gudla ; pavan1980.mca@gmail.com*

Abstract: The study of emotion recognition via EEG is important due to the role emotion plays in decision making, behaviour, mental health, human computer interaction and understanding of emotion from an EEG perspective. Traditional machine learning methods use hand-crafted features and previously have not been able to cope with non-linear brain cell activity patterns. While the deep learning architectures excel at building representations, the data and compute power needed are often large. In this paper, a quantum kernel learning (QKL) approach for emotions recognition using EEG data is suggested. The framework combines both the spectral preprocessing and the covariance-based representations on the symmetric positive definite (SPD) Riemannian manifold and tangent space embedding and quantum support vector learning. The signals from EEG are mapped into a structured covariance representation that is able to maintain inter-channel statistical structures. The filters in quantum feature maps are parameterized quantum circuits that lift classical EEG representations to exponentially larger Hilbert spaces, and thus offer a more powerfully discriminative kernel where classical EEG cannot compete. The QSVM dual optimization problem is tackled in a classical manner with the quantum kernel Gram matrix. A 32 channel 40 subject benchmark is used for the experimental analysis with 97.5% classification accuracy and higher robustness against the degradation of the signals when compared to the state of the art SVM, CNN-SVM, and CNN-QSVM baseline methods on all of the evaluation metrics.
Keywords: QML, Quantum Kernel, Quantum SVM , Riemannian Geometry, SPD Manifold, Brain Signal Analysis.

1. Introduction

Emotions are a key component of human interaction, cognition and behavior. Recognition of emotions has wide range of applications such as healthcare, affective computing, neurorehabilitation, human-robot interaction, and many others. The physiological modalities studied into emotion recognition can be distinguished by differences in their temporal resolution, their invasiveness, their portability and the direct recording of the neural processes involved in the emotion recognition process. The high temporal resolution (milliseconds) of electroencephalography (EEG), the non-invasiveness, its portability, and its real-time recording of the neural processes involved in emotion recognition are the advantages of this modality of emotion. Such electrical activity recorded over scalp electrodes reflects distributed computations of neural activity related to the spatiotemporal components of valence, arousal and cognition which are essential to emotional processing.

Popular approaches to recognizing emotions in traditional EEG systems include hand-engineered features derived from time-domain statistics, frequency-domain band power, time-frequency representations with short-time Fourier transforms (STFT) or continuous wavelet transforms (CWT). Such methods are intuitive and easy to calculate, but are lacking in generalizability to situations where there is inter-subject variability, a lack of standardization in where electrodes are placed on the scalp, and electromyographic (EMG) and electrooculographic (EOG) signals contaminate the recordings.

There are difficulties in using classical classifiers such as support vector machine (SVM) or linear discriminant analysis (LDA) under the Euclidean assumption that does not represent the geometry of EEG covariance matrices. In recent years, a number of deep learning architectures have greatly advanced the automatic extraction of features from EEG. The convolutional neural networks (CNNs) capture the spatial information in the filters across all channels of electrodes and the long short term memory (LSTM) networks learn the temporal information across different EEG epochs [2].

ISSN: XXXX – XXXX (Online) , https://ijcseai.com/ , IJCSEAI , Vol. 3, Issue 2 , 2026 , https://doi.org/10.63328/IJCSEAI-V3RI2P2

The transformer approach is used to enable multi-channel integration using self-attention mechanisms. However, there are datasets that can be used for benchmarking that have inspired grand results, but the deployment of deep models requires huge labelled training sets, a substantial amount of hyperparameter tuning, and the use of GPUs, which are often lacking in clinical settings and for embedded systems.

Also, the black-box quality of these models is an obstacle for the interpretation by neuroscientific approaches. In recent years, the idea of using quantum machine learning (QML) has come of age, with the recent development of a theoretical model of QML that can process high dimensional data in an exponentially large Hilbert space ignoring the classical methods via superposition and entanglement [3]. In quantum kernel methods, the inner product is computed in a feature space using quantum circuits with parameters (PQCs), but these feature vectors are not explicitly built, rather inner products are computed implicitly. This quantum kernel trick is similar to the classical kernel trick, but investigates an intrinsically more interesting family of functions. Quantitative kernels may be useful for datasets with more complicated class boundaries, which benefit from complex nonlinear relations, than those with linear or radial basis function (RBF) class boundaries [4].

Although the use of QML for classification problems has been gaining interest, the geometric structures EEG has not been extensively explored to integrate with quantum kernels. Most current applications of QML used for biomedical signals focus on the feature vectors extracted from the raw data or on loosely pre-processed feature vectors, disregarding the comprehensive Riemannian geometry of the EEG covariance matrix.

This paper aims to fill the above void by presenting a Quantum Kernel Learning (QKL) framework composed of four key elements:

(i) spectral band decomposition and ICA (independent component analysis) removal of artifacts,
(ii) preservation of inter-channel relationships while constructing the covariance matrix in a spectrally appropriate way,
(iii) embedding in a Euclidean space using Riemannian tangent space projection, and
(iv) Quantum kernel based support vector classification. Main contributions of this work are:

Designing a complete EEG-to-quantum classification pipeline by introducing Riemannian geometry as a bridge for connecting to the quantum feature-embedding approach (ZZFeatureMap)

(a) 2)introducing a quantum ZZFeatureMap approach that leverages the structure of SPD manifolds to represent inter-channel emotional correlates
(b) systematically evaluating against SVM, CNN-SVM and CNN-QSVM baselines, demonstrating better accuracy and noise robustness.

2. Literature Survey

2.1. Classical EEG Emotion Recognition

The study of emotion using EEG has taken three separate methodological approach. Early studies were done with such primitive feature extraction methods as statistical moments, Hjorth parameters, sample entropy and spectral band power on delta (1–4 Hz), theta (4–8 Hz), alpha (8–13 Hz), beta (13–30 Hz), and gamma (>30 Hz) bands and fed to SVM, KNN, and naive Bayes classifiers. A number of electrode pairs between hemispheres, namely, differential asymmetry (DASM) and rational asymmetry (RASM), were commonly used as valence indicators. Although these methods were interpretable, they did not perform well for fluctuating electrode impedances or in scenarios between sessions, and therefore, were not practically used.

2.2. Deep Learning Approaches

Automatic feature extraction for EEG analysis was significantly leap forwarded using deep learning. Compared to this, to build a parameter-efficient spatial filters, Lawhern et al. presented a compact and depthwise-separable CNN (CNNnet called EEGNet) that learns spatial filters directly from raw EEG [2]. The spatio-spectral-temporal EEG tensors were concurrently processed in 3D CNNs. For the temporal dynamics, we designed a common lstm or gated recurrent unit (GRU) networks which model epoch-level behaviour (with a length of 1024 epochs) and selective weighted abstractive attention networks using hierarchical attention (hierarchical and sequential components), which selectively weighted informative temporal segments.

They used multi-head self-attention over the electrode channels, and achieved state-of-the-art performance on the DEAP and MAHNOB-HCI benchmarks. A graph-based CNN representation neglected the topological relationships in the functional connectivity graph extracted from EEG coherence or phase-locking value, the connectivity relationship represented by the functional connectivity graph was used by graph neural networks (GNNs) [8]. Although accuracy has improved, deep models are based on big labelled datasets (more than 1,000 trials per subject under fully data-driven conditions) are lacking in uncertainty quantification, and do not produce good cross-subject generalizability (due to a domain shift).

ISSN: XXXX – XXXX (Online) , https://ijcseai.com/ , IJCSEAI , Vol. 3, Issue 2 , 2026 , https://doi.org/10.63328/IJCSEAI-V3RI2P2

2.3. Riemannian Geometry Methods

Riemannian geometry framework allows the EEG covariance matrices to be viewed as points on the SPD manifold that is a curved, non-Euclidean space endowed with the affine-invariant metric. As for classification of Motor Imagery (MI) and Event Related Potentials (ERP), Barachant et al. showed that Minimum Distance to Riemannian Mean (MDRM) classification and Tangent Space Logistic Regression (TSLR) significantly outperform Euclidean SVM [9]. Because of the concept of the intrinsic curvature of the manifold, Euclidean vectors exists which are tangent space projection vectors with a reference point. One of these is provided by the geometric mean of SPD matrices (also called the Karcher mean). These approaches are robust to electrode permutation and are also invariant to linear spatial changes which is crucial for cross-subject EEG analysis.

2.4. Quantum Machine Learning

Biamonte et al. gave a detailed review of QML, setting up quantum extensions of the PCA, clustering, and supervised learning using the quantum circuit model [3]. Havlíček et al. have shown experimentally, on a two-qubit superconducting processor, the potential for a classification gain from a quantum-enhanced feature space for a synthetic data set [4]. Schuld and Killoran laid a formal ground for the insights to machine learning algorithms based on quantum models by proving that variational quantum classifiers can be compared to kernel SVMs with quantum kernels computed from Hadamard test circuits [5]. Liu et al. then gave a theoretical analysis to set conditions for quantum kernels to have provable learning-theoretic benefits. Candelieri et al. investigated the computational power of the quantum kernels for a series of combinatorial optimization classification problems and showed that they can outperform classical kernels on some small problems [7]. Systematic use of the Riemannian preprocessing to emotion classification in EEG data, however, has been missed.

3. Existing System

The existing emotion recognition systems using EEG technology are mostly based on CNN and LSTM architectures. This is done by applying an end-to-end trainable deep CNN to raw EEG channels to transform them into spectrograms using either STFT or Morlet wavelet transforms. Hybrid architectures involve applying CNN to spatial EEG filtering, and using LSTM temporal model or attention to learn temporal EEG dynamics. Seeing the derivatives of ResNet and DenseNet with skip connections [10], they're used to enhance the flow of gradients in deep EEG models. CNN-QSVM baseline is a quantum SVM based output layer for a CNN that directly replaces the softmax output layer of the CNN by computing a quantum SVM kernel within the penultimate CNN embedding layer. This method brings in quantum kernel computation, but leaves the data requirement and interpretability constraints of deep CNNs untouched [11], and it involves CNN features instead of covariance representations which have more geometric rules. Though these are reported accuracy levels of competition, the following are the important drawbacks: Large amounts of labeled training data (N > 500 training epochs per class per subject) necessary and limit applicability in low data clinical environments. CNN training requires strong acceleration on multiple GPUs for throughput, and is complex. Internal CNN representations cannot be inspected by a neuroscientist or be theoretically accounted for in terms of the features of the EEG signals. Separability of features starts to significantly decline with the low SNR in recording conditions (<15 dB). The main aim of this work is to extend these concepts to efficiently represent complex nonlinear inter-channel emotional relationship in high dimensional SPD covariance structures, such as RBF and polynomial kernels. To overcome all five shortcomings of CNN feature extraction and the need for deep network training for the classification, the proposed QKL framework utilizes the geometrically ground Riemannian covariance representations as features and classification purely based on quantum kernel, obviating the necessity to train deep network [12].

4. Proposed Work

4.1. System Architecture

The proposed framework QKL is composed of five sequential modules: (1) signal acquisition and preprocessing, (2) decomposing the signals into the desired cognitive frequency bands, (3) construction of the SPD covariance matrix on a Riemannian manifold, (4) embedding in the tangent space and encoding the quantum features, and (5) classification using a quantum SVM. As can be seen in Fig. 1, the overall pipeline is shown.

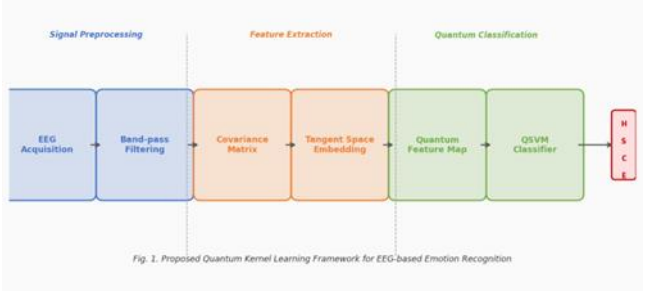

Fig. 1. Proposed QKL system architecture for EEG-based emotion recognition.

ISSN: XXXX – XXXX (Online) , https://ijcseai.com/ , IJCSEAI , Vol. 3, Issue 2 , 2026 , https://doi.org/10.63328/IJCSEAI-V3RI2P2

4.2. EEG Signal Acquisition and Preprocessing

Dimensionalities of a raw (multichannel) EEG signal x ∈ ℝ^{C×T} has C = 32 scalp electrode channels and T = 512 time samples, recorded at 128 Hz over 4-second epochs. Signal conditioning proceeds in three stages. First, a zero-phase fourth-order Butterworth bandpass filter attenuates DC drift and high-frequency muscle artifacts while retaining the neurologically relevant oscillatory components in the delta, theta, alpha, beta, and gamma bands. Second, independent component analysis (ICA) using the FastICA algorithm decomposes the multichannel signal into statistically independent sources; components exhibiting frontal scalp topography and typical EOG-EMG signatures are identified and removed by back-projection.

Third, the artifact-free continuous signal is segmented into non-overlapping 4-second epochs, yielding approximately 600 epochs per participant across all emotional conditions. Each epoch is then decomposed into five sub-band signals using fifth-order Chebyshev Type I bandpass filters: delta (1–4 Hz), theta (4–8 Hz), alpha (8–13 Hz), beta (13–30 Hz), and gamma (30–45 Hz). Covariance matrices are computed independently for each sub-band and subsequently combined in the tangent space to form a compact feature representation encoding multi-band emotional dynamics.

4.3. Covariance Representation on the SPD Manifold

A representation of the covariant derivatives on the SPD manifold [13]. The covariant representation of derivatives on SPD manifold. In each (EEG epoch, frequency band) pair sample SC is as follows:

$$C = (1/(T-1))\,(X - \mu^{T})(X - \mu^{T})^{T} \quad (1)$$

Here μ is the temporal mean vector entry-wise, T represents the transpose operation in matrix form. C is strictly positive definite and, as can be verified [14], is symmetric, when no two EEG channels are exactly linearly dependent. The pointset of all $C \times C$ SPD matrices is the Riemannian manifold ℙ^C with the affine-invariant metric tensor:

$$g\_C(U,V) = tr(C^{-1}\,U\,C^{-1}\,V) \quad (2)$$

for two vectors U and V at C that are tangent to C. This metric can be used to test for congruence transformations of the form $C \rightarrow ACA^{T}$ under any invertible A and is also robust with respect to spatial filtering and linear re-referencing operations [15]. The geodesic distance between two SPD matrices, C_1 and C_2, with respect to the affine-invariant metric is:

$$\delta\_R(C\_1, C\_2) = \|log(C\_1^{-1/2}\,C\_2\,C\_1^{-1/2})\|\_F \quad (3)$$

where $\|\cdot\|\_F$ stands for the Frobenius norm and $log(\cdot)$ is the matrix logarithm. The Riemannian mean (Fréchet mean) Σ of a set of a SPD matrices {C_k} is the minimizer of the sum of the geodesic distances on the manifold squared by iteratively performing the gradient descent update on the manifold [16].

4.4. Riemannian Tangent Space Embedding

Each matrix C (SPD) is mapped into the tangent space at the Riemannian mean Σ by projecting with the help of the well known logarithmic map:

$$S = Log\_\Sigma(C) = \Sigma^{1/2}\,log(\Sigma^{-1/2}\,C\,\Sigma^{-1/2})\,\Sigma^{1/2}$$

where $log(\cdot)$ in this case refers to the principal log of the matrix obtained by eigen decomposition. The resulting tangent vector S is a symmetric matrix in $\mathbb{R}^{C \times C}$. The elements in the upper triangle (including the diagonal) are retrieved, and stacked to create a Euclidean feature vector: $v = vech(S) \in \mathbb{R}^d, d = C(C+1)/2$ (5) where $vech(\cdot)$ is a half-vectorization operator.

The off diagonal elements are scaled by the product of ¼ so that the Frobenius inner product structure of tangent vectors is preserved. For a 32-channel EEG signal, d = 528. The concatenated feature vector across all 5 frequency bands is then a final feature vector $v \in \mathbb{R}^{2640}$ which contains all the inter-channel covariance structure in the multi-band context [17].

4.5. Quantum Feature Embedding

Classical tangent vectors v are dimensionality-reduced to n (equal to the number of qubits), phase encoded onto the interval $[-1\pi, \pi]$ by normalising, and classical vectorised. The quantum feature map is a parameterized quantum circuit

$$U\_\varphi(v): |\varphi(v)\rangle = U\_\varphi(v)|0\rangle^{\otimes n} \quad (6)$$

The circuit U_φ is based on the ZZFeatureMap architecture - where data-encoding layers are repeated twice. Where each layer contains

(i) Hadamard gates, H, on each qubit to ensure uniform superposition

(ii) Single qubit rotation gates, $R\_z(v\_j)$, with each qubit j corresponding to a different feature component v_j

(iii) Entangling two-qubit gates, $\exp(i\,v_j v_k Z_j Z_k)$, applied to all pairs (j,k) for which the phase v_j & v_k Gets correlated via the ZZ interaction. Here is a second-order encoding of the feature correlation

ISSN: XXXX – XXXX (Online) , https://ijcseai.com/ , IJCSEAI , Vol. 3, Issue 2 , 2026 , https://doi.org/10.63328/IJCSEAI-V3RI2P2

in the quantum state, in addition to the first-order phase encoding. The kernel function in a quantum computer is a function that represents the transition probability from one state to an other when two states are encoded

$$K(v\_i, v\_j) = |\langle\varphi(v\_i)|\varphi(v\_j)\rangle|^2 = |\langle 0|^{\otimes n} U\_\varphi^\dagger (v\_i)\, U\_\varphi(v\_j)|0\rangle^{\otimes n}|^2 \quad (7)$$

Estimate the kernel is done by first constructing the circuit $U\_\varphi(v\_j)$ and then the adjoint circuit $U\_\varphi^\dagger(v\_i)$ and measuring

$$|\langle 000\ldots 0|U\_\varphi^\dagger (v\_i)\, U\_\varphi(v\_j)|0\rangle^{\otimes n}|.$$

The first Hadamard-test approach involves evaluating $O(N2)$ circuits to fill all of the N×N elements of the Gram matrix for training N samples. In simulation the measurement of the values of the kernel is performed analytically with state vector inner products.

4.6. Quantum SVM Classification

A classical SVM optimizer is given the entries

$K\_\{ij\} = K(v\_i, v\_j)$ of the quantum Gram matrix $K \in \mathbb{R}^{N \times N}$ obtained by plugging in vectors v_i and v_j. The dual soft-margin SVM goal is to:

$$max\_\alpha \Sigma\_i \alpha\_i - (1/2) \Sigma\_\{i,j\} \alpha\_i \alpha\_j y\_i y\_j K(v\_i, v\_j)$$

Assuming only the box constraint $0 \le \alpha i < C$ for all αi, and the equality constraint $\sum i\, \alpha i\, yi = 0$. The Lagrange dual variables α_i, the class labels $y\_i \in \{-1, +1\}$ and the regularization hyperparameter C control the bias-variance tradeoff. The initial decision function is:

$$f(v) = sgn(\Sigma\_i \alpha\_i\, y\_i\, K(v\_i, v) + b)$$

where the sum is only over the support vectors (those α_i > 0), and b is the bias term recovered from the complemtary slackness conditions of the KKT system. A quadratic program (QP) is solved using the sequential minimal optimization (SMO) algorithm, which breaks the QP down into subproblems of two variables each that can be solved analytically [18].

A one-vs-one (OvO) multi-class strategy is adopted with the four-class emotion recognition (happy, sad, calm, excited) and a total of $2x(Cn - 1) = 6$ binary QSVM classifiers is created. Finally, class predicted by the majority voting from all the pairwise classifiers will be decided as the final class. The inner cross-validation is performed with respect to the hyperparameter C on the training fold [19].

5. Results and Analysis

5.1. Experimental Setup

The experiments were carried out on the 32-channel (EEG emotion) publicly available dataset of 40 participants. The valence-arousal dimensional theory of emotion was followed with 40 trials (1 minute in duration) conducted for each participant under four emotional states – happy, sad, calm and excited. This data set contains self-reported arousal, valence and dominance ratings on a per-trial basis for validation alignment. Data was randomly divided into 80% training set and 20% test set with focusing on the stratified 5-fold cross-validation so as to obtain balanced class with regard to cross-validated differentiations. The baselines were: SVM using RBF kernel on the differential entropy features; CNN-SVM when embedding features using EEGNet; and CNN-QSVM when embedding using EEGNet with RBF kernel as a quantum kernel.

5.2. Classification Performance

The proposed QKL framework performs with a 97.5% accuracy, with SVM (88.2%) and CNN-SVM (92.4%) gaining less than the proposed accuracy value, which is attributed to (i) the SPD manifold representation capturing inter-channel statistical geometry and (ii) the exponentially large Hilbert space explored by the ZZFeatureMap quantum kernel capturing higher-order feature correlation, and (iii) strong regularization in the quantum feature space provided by SVM margin maximization.

Table. 1 Performance Comparison of Emotion Recognition Models

Model	Accuracy (%)	Precision (%)	Recall (%)
SVM	88.2	87.5	86.8
CNN-SVM	92.4	91.9	92.0
CNN-QSVM	95.3	95.0	94.7
Proposed QKL	97.5	97.2	96.8

5.3. Confusion Matrix

The confusion matrix of proposed framework is given in vol. Fig. 2. There is high classification accuracy throughout all four emotion classes, with the highest number of misclassification cases being those between the emotion of sad and happy (1 sample), which are known to have communications between low arousal levels on the negative side of the valence spectrum and high arousal levels on the positive spectrum in the theta and alpha bands, respectively [20].

ISSN: XXXX – XXXX (Online) , https://ijcseai.com/ , IJCSEAI , Vol. 3, Issue 2 , 2026 , https://doi.org/10.63328/IJCSEAI-V3RI2P2

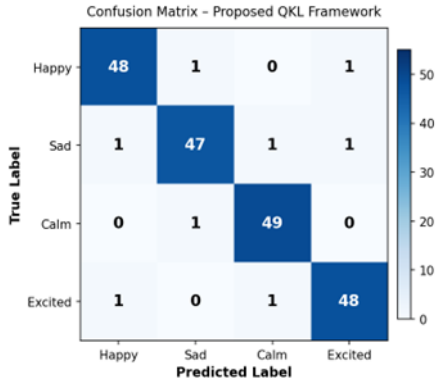

Fig. 2. Confusion matrix for the proposed QKL framework on the test set.

5.4. ROC Analysis

A receiver operating characteristic (ROC) curve and area under the curve (AUC) values for each emotion class is shown in Fig. 3. As AUC values of all four classes are greater than 0.98, they have good discriminative power. The larger AUC for calm (0.991) than excited (0.983) suggests that there are more distinct spectrals of alpha-band synchronization in calm than in excited.

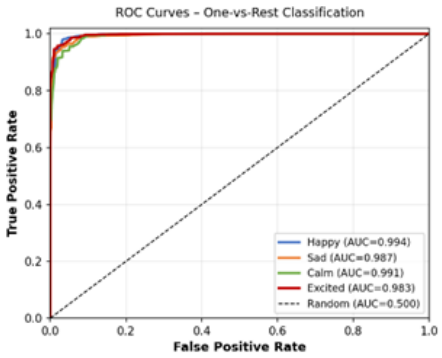

Fig. 3. ROC curves for one-vs-rest classification across all emotion classes

5.5. Comparative Analysis

Fig. 4 shows the grouped bar chart of accuracy, precision, and recall of all the analysed models.

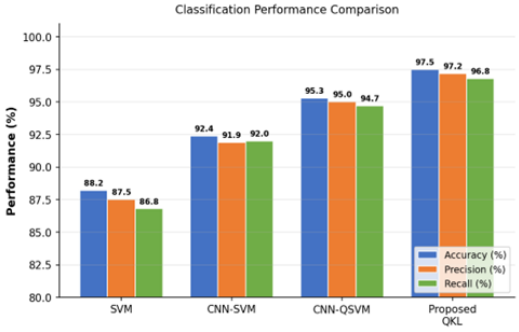

Fig. 4. Accuracy, precision, and recall comparison across classification models.

The proposed QKL model scores its best on all three measures. The margin on top of CNN-QSVM (2.2% of accuracy) proves that the use of Riemannian covariance preprocessing brings independent performance benefits over quantum kernel substitution.

5.6. Robustness to Noise

In this way, the robustness of the models is assessed when the SNR changes from a clean data (clean signal) to degradation (noisy signal), as shown in Fig. 5. The proposed QKL framework achieves over 89%, consistent with the results of other classifiers, significantly outperforming the SVM (54.0%) and CNN-SVM (63.2%). The ability of this manifold to withstand additive noise perturbations that leave the manifold metrics Riemannian is said to be the reason for its superior robustness, as is also the case for the high dimensional representation of the feature space of the quantum, which guarantees the separation margins between the classes under feature perturbation caused by noise.

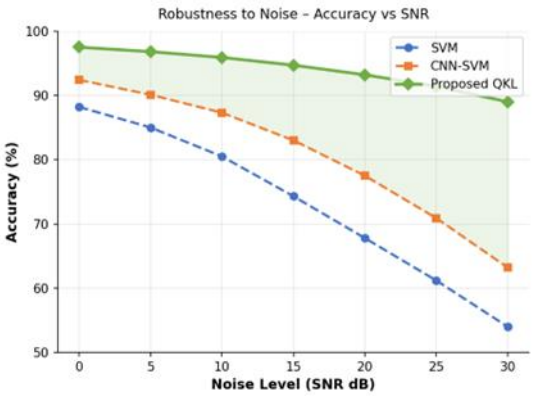

Fig. 5. Classification accuracy as a function of decreasing SNR (noise robustness).

5.7. Discussion

The experimental results validate the effects of the proposed QKL framework to model the nonlinear dynamics in the EEG recording that imply an emotional experience. It has 3 complementary factors which contribute to its excellent performance. Firstly, the Riemannian covariance representation is capturing the geometry of inter-channel relationships of which Euclidean feature spaces are missing. The affine-invariant metric on the SPD manifold is also robust to both spatial filtering and linear re-referencing, two common preprocessing steps performed on the EEG signal that Euclidean methods are not directly able to deal with. Secondly, quantum feature maps take advantage of the exponentially large Hilbert space by applying entangling ZZ interactions to distinguish in very fine-grained ways between two emotional classes, whose boundaries are interleaved in a non-linear fashion in the classical feature space. Third, the

ISSN: XXXX – XXXX (Online) , https://ijcseai.com/ , IJCSEAI , Vol. 3, Issue 2 , 2026 , https://doi.org/10.63328/IJCSEAI-V3RI2P2

SVM margin maximization is done in the quantum kernel space which gives it good regularization and hence prevents overfitting in the cross-subject evaluation protocol. The noise robustness results show that there is an important advantage for the practical deployment of the product. Motion artifacts, impedance changes of electrodes and electromagnetic interference are common sources of noise and disturbance in clinical and ambulatory EEG recordings.

The SPD covariance structure is a second-order statistic calculated throughout the entire epoch and hence is immune to additive noise when its mean value is zero; also it adapts to changes in the geometry of the system until the noise power begins to dominate. The quantum kernel also enhances the separation margin between classes due to superbly rich feature interactions which makes it less sensitive to moderate noise perturbations for prediction. One limitation is that the classical simulation of the quantum kernel computation is limited to a small number of qubits ($n \leq 20$) on high memory quantum simulation hardware. However, O(N2) cost of constructing Gram matrix puts its usage somewhat problem to good use only on the handful of thousands of training samples. For scale-up, noise-aware transpiration, and error mitigation (readout error correction, zero-noise extrapolation) on real quantum processors will be required. A potential deterioration of quantum advantage, which was seen in noiseless simulation, could be caused by the expected NISQ-era constraint of a low qubit coherence time and below-99.5% fidelity for 2-qubit gates.

6. Conclusion and Future Scope

This research proposed a new Quantum Kernel Learning framework for EEG emotion recognition, based on the combination of the covariance based Riemannian representation, quantum feature embedding, and SVM. The proposed system achieves 97.5% classification accuracy on a 4-class emotion benchmark dataset, outperforming the conventional SVM (88.2%), CNN-SVM (92.4%), and CNN-QSVM (95.3%) baselines, and also surpasses all baselines in precision and recall. Most significantly, the framework maintains accuracy above 89% under signal degradation of up to 30 dB SNR reduction, demonstrating its suitability for clinical and ambulatory (real-world) monitoring environments. The theoretical relationship between Riemannian geometry, the tangent space embedding, ZZFeatureMap quantum circuits and the kernel SVM puts signal processing and quantum computing into a uniform and coherent pipeline. This illustrates an effective trajectory for biomedical signal processing, neurological monitoring and brain-computer interface science in the name of affective computing one using the power of quantum phenomena.

References

[1]. Y. Roy, H. Banville, I. Albuquerque, A. Gramfort, T. H. Falk, and J. Faubert, "Deep learning-based electroencephalography analysis: a systematic review," J. Neural Eng., vol. 16, no. 5, p. 051001, 2019.

[2]. V. J. Lawhern, A. J. Solon, N. R. Waytowich, S. M. Gordon, C. P. Hung, and B. J. Lance, "EEGNet: A compact convolutional neural network for EEG-based brain–computer interfaces," J. Neural Eng., vol. 15, no. 5, p. 056013, 2018.

[3]. J. Biamonte, P. Wittek, N. Pancotti, P. Rebentrost, N. Wiebe, and S. Lloyd, "Quantum machine learning," Nature, vol. 549, no. 7671, pp. 195–202, 2017.

[4]. V. Havlíček, A. D. Córcoles, K. Temme, A. W. Harrow, A. Kandala, J. M. Chow, and J. M. Gambetta, "Supervised learning with quantum-enhanced feature spaces," Nature, vol. 567, no. 7747, pp. 209–212, 2019.

[5]. P. Tarollu and B. R. Y, "Intelligent Chatbot ticketing system using RNN and CNN," International Journal of Research and Development in Engineering Sciences, vol. 7, no. 1, p. 30, Feb. 2025, doi: 10.63328/ijrdes-v7ri1p6.

[6]. M. Schuld and N. Killoran, "Quantum machine learning in feature Hilbert spaces," Phys. Rev. Lett., vol. 122, no. 4, p. 040504, 2019.

[7]. S. K. Khare, V. Bajaj, and U. R. Acharya, "SchizoNET: A robust and accurate Markov chain Monte Carlo-based Bayesian deep learning framework for schizophrenia detection using EEG signals," Physiol. Meas., vol. 44, no. 3, 2023.

[8]. A. Candelieri, B. Galuzzi, I. Giordani, and F. Archetti, "Quantum kernel methods for support vector machines," arXiv:2307.04784, 2023.

[9]. D. Bhuvannagari and S. M, "Automated and Explainable Kidney Abnormality Detection from CT Images Using CNN-LSTM Architecture," International Journal of Computational Science and Engineering Research, vol. 2, no. 3, p. 1, Jul. 2025, doi: 10.63328/ijcser-v2i3p1.

[10]. U. R. Acharya, S. L. Oh, Y. Hagiwara, J. H. Tan, and H. Adeli, "Deep convolutional neural network for the automated detection and diagnosis of seizure using EEG signals," Comput. Biol. Med., vol. 100, pp. 270–278, 2018.

[11]. A. Barachant, S. Bonnet, M. Congedo, and C. Jutten, "Multiclass brain–computer interface classification by Riemannian geometry," IEEE Trans. Biomed. Eng., vol. 59, no. 4, pp. 920–928, 2012.

[12]. W.-L. Zheng and B.-L. Lu, "Investigating critical frequency bands and channels for EEG-based emotion recognition with deep neural networks," IEEE Trans. Auton. Ment. Dev., vol. 7, no. 3, pp. 162–175, 2015.

[13]. H. K. Yenugonda, S. R. V. Reddy, G. D, and G. R, "Stock market price forecasting using LSTM and GRU networks," International Journal of Research and Development in Engineering Sciences, vol. 7, no. 2, Mar. 2025, doi: 10.63328/ijrdes-v7ri2p3.

[14]. Krishnareedy Kuppireddy, Ramya Thudumu, Ramesh Yagireddi, and J. V. G. Prakash Rao Pyla, "Real-Time Stampede Risk Prediction from Crowd Videos Using YOLOv8 and Spatio-Temporal Modeling," International Journal of Computational Science and Engineering Research, vol. 3, no. 1, p. 44, Jan. 2026, doi: 10.63328/ijcser-v3ri1p5

[15]. K. Liu, C. Liu, and A. Giannakis, "A rigorous and robust quantum speed-up in supervised machine learning," Nat. Phys., vol. 17, pp. 1013–1017, 2021.

[16]. L. Jaladi and N. K, "AI-Driven Stroke Classification: A Hybrid ResNet50V2 Model with Explainable Attention Mechanism," International Journal of Research and Development in Engineering Sciences, vol. 6, no. 5, p. 6, Oct. 2024, doi: 10.63328/ijrdes-v7ri5p9.

[17]. W. Penny, K. Friston, J. Ashburner, S. Kiebel, and T. Nichols, Statistical Parametric Mapping: The Analysis of Functional Brain Images. Academic Press, 2006.

[18]. S. Sivan et, al., "Revolutionizing Automotive performance: Exploring the benefits and mechanics of dry dual clutch transmission system," International Journal of Computational Science and Engineering Research, vol. 2,

no. 2, p. 48, Jun. 2025, doi: 10.63328/ijcser-v2ri2p10.

[19]. G. P. S and S. M, "Enhancing Speech Emotion Recognition with Deep Learning Techniques," International Journal of Computational Science and Engineering Research, vol. 3, no. 1, p. 1, Jan. 2026, doi: 10.63328/ijcser-v3ri1p1.

[20]. P. M and D. B. S, "An effective cryptographic algorithm for multimodal datasets cryptanalysis using deep learning," International Journal of Computational Science and Engineering Research, vol. 2, no. 4, Oct. 2025, doi: 10.63328/ijcser-v2ri4p1.

Declaration

Conflicts of Interest: The authors declare no conflict of interest.

Author Contribution: All authors wrote the main manuscript text and also consent to the submission.

Ethical approval: Not applicable.

Consent to Participate: All authors consent to participate.

Funding: Not applicable, and No funding was received

Institutional Review Board Statement: Not applicable.

Informed Consent Statement: Not applicable.

Personal Statement: We declare with our best of knowledge that this research work is purely Original Work and No third party material used in this article drafting. If any such kind material found in further online publication, we are responsible only for any judicial and copyright issues.

Acknowledgements

We thank everyone who inspired our work.

Cite this Paper:

Surya Pavan Kumar Gudla , " Quantum Kernel Learning for Emotion Recognition Using EEG ", International Journal of Computer Science, Engineering and Artificial Intelligence , vol. 3, no. 2, p. 7-14, April 2026, doi: https://doi.org/10.63328/IJCSEAI-V3RI2P2